Advanced seasonal predictions for vine management based on bioclimatic indicators tailored to the wine sector

Chihchung Chou [a,*], Raül Marcos-Matamoros [a,b], Lluís Palma Garcia [a], Núria Pérez-Zanón [a], Marta Teixeira [c], Sara Silva [c], Natacha Fontes [c], Antonio Graça [c], Alessandro Dell'Aquila [d], Sandro Calmanti [d], Nube González-Reviriego [a]

[a] *Earth Sciences Department, Barcelona Supercomputing Center - CNS, Plaça d'Eusebi Güell, 1-3, Barcelona 08034, Spain*
[b] *Department of Applied Physics, University of Barcelona, Av. Diagonal 647, Barcelona 08028, Spain*
[c] *Sogrape Vinhos SA, Rua 5 de outubro, 4527, 4430-852 Avintes, Portugal*
[d] *ENEA, SSPT-MET-CLIM, CR Casaccia, Via Anguillarese 301, 00123 Rome, Italy*

ABSTRACT

The potential increase in the adoption value of seasonal forecasts is spotlighted in this paper by introducing observation-forecast blending for wine-sector indicators over the Iberian Peninsula. The predictions of six bioclimatic indicators (temperature and precipitation based) considered highly important from the perspective of wine-sector users were prepared for each month of the growing season and combined with previous observations as the indicator period progresses. The performance of this approach was then assessed with Pearson's correlation coefficient and Fair Ranked Probability Skill Score (FRPSS). The results show a marked increase in the skill metrics during the growing season from the early combinations for all the indicators. This progressive improvement of the forecasting skill offers the users an opportunity to ponder anticipation and confidence in their decisions and, thus, facilitate the future uptake of seasonal forecasting in their decision planning.

Practical Implications

Climate change poses a major challenge to wine grape growing, and thereby unprecedentedly affects the winemaking industry in the Mediterranean region. For example, the traditional match between locations and grape varieties was found not to be as suitable as before in terms of its climate in the condition of the observed global warming. As such, policymakers in the sector may have to annually estimate the potential benefits and costs of shifting the regulated limits of the producing areas to match the climate required for their varieties. Alternatively, adjusted regulatory strategies are required to fit business models into the forthcoming weather by changing modes of production or even the categories of viticultural products according to the forecast weather. This might mean a relevant change in the markets and consumer preferences too. In addition, reliable and advanced climate forecasts in seasonal timescale would also need to be reconsidered because the management of manpower and vineyard and winery logistics would be more challenging if unprecedented climate extremes and severe interannual variability became a new normal.

Seasonal forecasts have been a readily useful adaptation tool with a wide range of applications in fields, including agriculture (Vajda and Hyvärinen, 2020). By co-developing the tailored bioclimatic indicators based on seasonal forecasts together with the users, the customized climatic information could assist decision-making months ahead of the critical periods of the growing season. However, seasonal forecasts with insufficient skills would prevent users from applying it in their decision workflow. Unfortunately, the skill of the seasonal forecasts was rather limited outside of the tropics (Doblas-Reyes et al., 2013). Consequently, we merged forecasts with observations (i.e., the 'blending' strategy) in the structure of the bioclimatic indicators. By applying this methodology, the potential increase in skill could allow the users/practitioners to achieve an acceptable trade-off between anticipation and skill and, hence, to spot the best timing for a decision to be made.

Remarkably, our results show that this 'blending' approach

implies a steady increase in both of the skill metrics from the early stages of the growing season. Specifically, the Growing Season Temperature (GST) and Growing Degree Days (GDD) show the best skill in the early months among the six indicators. As for the precipitation-derived ones, the Spring Total Precipitation (SprR) prediction tended to be more skilful than Harvest Total Precipitation (HarvestR) after a one-month observation was included. Moreover, the spatial distribution of their performance also varies: the south of the Iberian Peninsula (IP) attained more skill for SprR while it was easier to forecast HarvestR in the north. Regarding the two heat stress indicators (i.e., number of heat stress days - SU35 and Warm Spell Duration Index - WSDI), the progressive increase in skill for SU35 was focused on the southern part of the IP while the improvement was more widespread for WSDI. Furthermore, WSDI began to be skilful approximately-one month earlier than SU35.

In summary, the practical implication of this paper is that the progressive increase in the skill attained with the 'blending' strategy would ultimately empower decision- and policy-maker to use seasonal forecasts in the most favorable moment considering their risk profile.

Data availability

Data will be made available on request.

Introduction

The Mediterranean region is the historical cradle of winemaking (Comité Européen des Entreprises Vins, 2015) and the European Union, its major producer, contributes to more than 65 % of the global wine supply (OIV, 2016). However, since grape growing is sensitive to climate conditions (Camps and Ramos, 2012), current and future climate conditions pose a major challenge to this sector, especially as unprecedented extreme events become more frequent (Diffenbaugh et al., 2017). For instance, Jones and Alves (2012) showed that currently observed global warming has already shifted the grape-growing landscape by making the traditional regions hotter and/or drier and, simultaneously, benefiting other areas that have become more suitable for this activity. Moreover, Fraga et al. (2014b) also explored this behavior at the regional level by studying these effects in one of the historical Portuguese wine-making regions, the Douro Valley. Actually, this climatic pressure (Blanco-Ward et al., 2019) has been spotlighted by several studies stating that by 2070 the Douro Valley would shift 4–5 categories (out of 16) towards warmer and drier conditions (Fraga et al., 2014b; Koufos et al., 2014).

Consequently, climate change has been an important footprint in wine-related decision-making (highlighting the overall need to adapt strategically to climate change). For example, Jones et al. (2005) found more significant warming for seasonal minimum temperatures than for the maximum ones and strong correlations (between -0.4 and -0.8) between the phenological and climatic variables (i.e., maximum temperatures) in the past five decades. Furthermore, the change rate of the relevant maturity date was up to three days per year (Petrie and Sadras, 2008; Tomasi et al., 2011). As such, an advanced and trustworthy seasonal prediction can better inform all the related decisions when the harvesting season keeps changing.

Although physiological adaptations and genetic selection have already been explored to cope with the forthcoming severe heat stress (Venios et al., 2020), the application of seasonal forecasts is one of the powerful adaptation tools as seen in the fields such as renewable energies (Torralba et al., 2017), water resource management (Marcos-Matamoros et al., 2017; Emerton et al., 2018) and agriculture (Vajda and Hyvärinen, 2020; Hansen et al., 2011; Winsemius et al., 2014; Malheiro et al., 2010).

In this framework, the combination of seasonal forecasts with bioclimatic indicators tailored for the wine sector could assist decision-making months ahead of the critical periods (like the growing season) of the year. For this reason, the development of climate services co-designed with the end-users maximizes the advantages of seasonal predictions on specific bioclimatic indicators (Soares et al., 2019; Marcos-Matamoros et al., 2020). A recurrent demand to enable the application of seasonal forecasts in the users' decision workflow is having predictions with high enough skill (aimed at risk aversion, as described in Giuliani et al., 2020). Although the level of skill needed depends on users and their decisions, the skill of the seasonal forecasts outside the tropics was rather limited (Doblas-Reyes et al., 2013, and references therein). The solution proposed in this paper aims to merge observations and forecasts in the bioclimatic indicator structure ('blending' strategy). This strategy is valuable because it permits the users to achieve a trade-off between anticipation and skill to identify when a decision can be safely triggered. To our knowledge, there are still no studies analyzing this combination of bioclimatic indicators specific to the wine sector together with the use of seasonal forecasts and the 'blending' strategy.

Therefore, our target is to understand the forecast potential of a range of sectoral bioclimatic indicators by portraying the balance between skill and anticipation. To do so we have studied predictions initialized at each month of the growing season (from April to October) over the IP and integrated them with observations as the growing season progressed. From the climate services perspective, this post-processing of climate forecasts (e.g., calculations of bioclimatic indicators) needs a wide range of efficient and appropriate software: firstly, it should be able to take advantage of the available computational resources (e.g., parallel computing) given the considerable amounts of daily data involved in this kind of analysis; secondly, by confirming the compatibility with existing software (e.g., for the skill scores computation); and, finally, being flexible to adapt the calculation to different regions, systems and time periods would be critical too. To fulfill these needs, this work also introduced the newly released CSIndicators R-package for the calculation of the selected indicators (see Table s1 for the details of the functions, Pérez-Zanón et al., 2021c).

The paper is organized as follows. In the next section, we introduce the used data sets and the spatial domain followed by the definitions of the selected bioclimatic indicators and the 'blending' scheme explained in section 3. After that, section 4 presents the results including the performance of the forecast indicators for all the initialization dates. Finally, the key outcomes of the paper are summarized in section 5.

Data and spatial domain

Seasonal prediction model

In this work, the daily temperature (mean, maximum and minimum) and precipitation from the European Center for Medium-Range Weather Forecasts (ECMWF) SEAS5 predictions (hindcast from 1993 to 2016) have been used. The data was downloaded from the Climate Data Store (Raoult et al., 2017) of the Copernicus Climate Change Service (C3S-CDS). SEAS5 is the fifth-generation seasonal forecast system of the ECMWF. The Copernicus version of the SEAS5 uses the Integrated Forecast System (IFS) Cycle 43r1 and provides a 25-member ensemble of a variety of Essential Climate Variables (ECVs) at 1-degree spatial resolution and up to 7 months ahead (Johnson et al., 2019; Manzanas et al., 2019; Gubler et al., 2020; Weisheimer et al., 2021).

Reference dataset

The reference dataset, downloaded from the CDS too, comes from the ECMWF ERA5 reanalysis with a horizontal resolution of 31 km (Hersbach et al., 2018). It provides a variety of land, atmospheric and oceanic climate variables from the year 1979 onwards. In some comparison
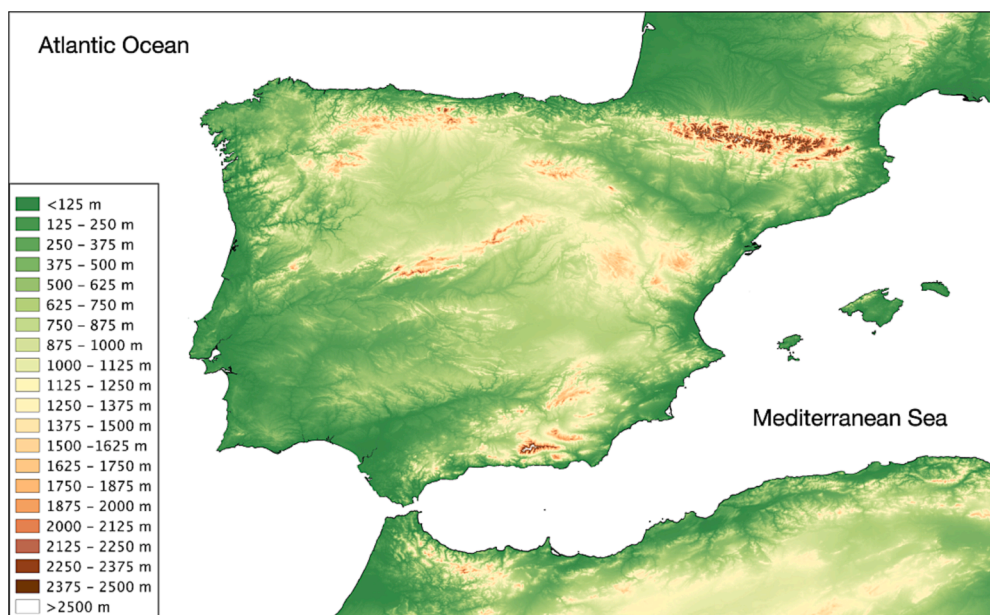
Fig. 1. Iberian Peninsula's relief. Elaborated from GMTED2010 (Danielson and Gesch, 2011).

studies with station-based observational data sets, data from ERA5 reanalysis generally reproduced the rainfall patterns at climatic scales (annual cycle of monthly mean) but in some places it tended to over-estimate precipitation all year round (such as in northern Europe and southern regions of central Europe, Bandhauer et al., 2022 and North America, Xu et al., 2019). As for surface air temperature and the wine-sector indicators (i.e., SU35 and WSDI) derived with daily temperature maximum, station-based observational data provided by SOGRAPE (our end-user, see the description in section 3.1) showed that ERA5 was generally comparable with other reanalysis data sets such as E-OBS in terms of RMSE and correlation (Sanderson et al., 2019). The variables used include daily precipitation and temperature (maximum, mean and minimum) for the same period as the SEAS5 prediction (1993–2016, the hindcast period). This product is based on the IFS Cy41r2 including 137 levels in the atmosphere on a regular longitude-latitude grid (Hersbach et al.,2020).

ERA5 reanalysis data were used to adjust the bias of SEAS5 prediction and it was also the reference dataset when computing the forecasting skill metrics such as the Pearson's correlation coefficient and the Fair Ranked Probability Skill Score (FRPSS).

Spatial domain

The spatial domain of this study is one of the most important wine-producing areas in the Mediterranean region: the IP encompasses widespread viticultural areas in Portugal (31 regions, see https://www.ivv.gov.pt/np4/regioes/) and Spain (70 regions) (see https://www.foodswinesfromspain.com/). IP is located in south-western Europe and it is mainly surrounded by water bodies: the Mediterranean to the east and south-east; and the Atlantic Ocean to the north, north-west and south-west (see Fig. 1). To its north-east, it is connected to the rest of Europe through the Pyrenees. Its geographical situation, orography and the influence of surrounding water bodies determine a variety of climatic regimes that imprints characteristic trademarks to its viticulture regions (Fraga et al., 2014a).

In this area the co-variability of climatic variables (e.g., temperature and precipitation) depicted varying structures due to different large-scale patterns' composites (Rodrigo et al., 2021; Meehl and Tebaldi, 2004) in addition to the local-scale land–atmosphere interactions (Vidale et al., 2007; Fischer et al., 2007). For instance, it has been studied that the North Atlantic Oscillation (NAO) is one of the

predominant large-scale atmospheric modes influencing the climatic variability over the Iberian Peninsula, in particular winter precipitation over the western IP (Goodess and Jones, 2002; Trigo et al., 2004).

Methodology

Definition of bioclimatic indicators

Through the process of co-development with our end-users (SOGRAPE), we selected six bioclimatic indicators that are highly relevant to vine growth, grape yields and harvest dates (see Jones and Davis 2000, Jones and Alves 2012 and the list of indicators in Table II & IV of Fontes et al., 2016). SOGRAPE is a large wine company based in Portugal, managing vineyards and producing wines across five countries on three continents. It has invested significantly in climate science, both by equipping itself with a network of vineyard-based weather stations providing quality data since 2011 and by partnering in several climate science projects at the national and international levels.

On the one hand, this group of indicators was settled given that the temperature-derived indicators fully cover the period of interest (i.e., the growing season of grapevines). On the other hand, another important ECV, precipitation, was also used to estimate the wetness in the early and harvesting stages of the season, which were considered in two bioclimatic indicators used. Besides, it is worth noting that indicators relating to winter rainfall were not selected in this work considering the higher risks and potential losses caused by (high) rainfall in the late spring and during the harvest period (Sanderson et al., 2022).

These indicators are Spring Total Precipitation (SprR), Harvest Total Precipitation (HarvestR), Growing Season Temperature (GST), Growing Degree Days (GDD), number of heat stress days (SU35) and Warm Spell Duration Index (WSDI). All the formulas can be found in the supplementary material along with the corresponding functions in the CSIndicators R-package. In the following sections, they are categorized into three subsections according to the climate variable used and their definitions are summarized along with the meaning and importance in terms of viticulture management. Note that the seasons considered by all the following indicators are for the Northern Hemisphere.

Precipitation-related indicators

SprR represents the accumulated precipitation during springtime, referring to the period from 21st April to 21st June. In dry springs, there

will be a lower pressure of fungal diseases which, in turn, reduces costs related to the application of protective treatments/operations. In addition, the amount of precipitation during this period also affects the level of vigor, translating to the grapevine's water requirements and the quality of grapes.

In addition to spring precipitation, the accumulated rainfall in the harvest season, referring to the HarvestR indicator, is also important and this indicator is defined as the total precipitation from 21st August to 21st October. Moderate precipitation in summer, for example, can be beneficial because the cost for additional irrigation is avoided while ensuring a correct hydric state of grapevines. However, heavy rainfall during this period increases the fungal (*Botrytis*) infection risks, spoiling berries, and favoring the development of acetic and gluconic acids (among other compounds) that are detrimental to wine quality (Toit and Pretorius, 2002). Furthermore, if heavy rainfall is received during the harvest period, there will be potential disruptions for both vineyard and winery logistics (e.g., labour availability and scheduling), translating to higher costs.

Average temperature-related indicators

GST is the 7-month average of daily mean temperatures over the entire growing season from 1st April to 31st October. Since many of the most used grapevine varieties have been classified according to their optimum ranges of GST, this intuitive indicator is frequently used in the wine sector (Karoglan et al., 2018) at least in two ways. On the one hand, for a given location, the anomalies in the predicted GST can be used to plan the possible outcomes of the season in terms of grape quality and phenology. On the other hand, according to the suitable range of GST for a specific variety, the end-user can look for the best locations to grow specific grapevine varieties and rootstocks. In this context, beyond the seasonal timescale, the GST indicator also helps to determine/adjust the varieties for the predicted climate of the coming years/decades.

The GDD indicator is defined as the daily sum of mean temperature exceeding 10 °C over the entire growing season from April to October. Although this indicator is highly correlated with GST, it is better linked with plant phenology and, hence, is often used for strategic decision-making (i.e., monitoring the phenological phases and the emergence of plagues). Like the GST indicator, GDD also characterizes the wine-growing regions by the suitability to a given type of grapes/wines.

Maximum temperature-related indicators

WSDI is the total count of days with ≥ 6 consecutive days when the daily maximum temperatures exceed the 90th percentile for the period from 1st April to 31st October. The WSDI compares the prediction with the 90th percentile in the observation with the additional criterion of the length of 'warm spell'. As such, WSDI signals the span of a heatwave, which is associated with water depletion, flowering disruption, dehydration and scalding of berries and leaves.

SU35 is the total count of days when daily maximum temperatures exceed 35 °C over the growing season. For grapevines, 35 °C is the average threshold for photosynthesis to stop occurring. Above this temperature, the plant closes its stomata, so the SU35 indicator hints at the number of days in which the photosynthesis process would be limited. Furthermore, if this situation continues after veraison (i.e., the moment when the grape berries stop vegetative growth, change their colors and mature), maturation will be arrested for as long as the condition holds. In such circumstances, all essential components for grape and wine quality such as sugar, polyphenol and aroma precursor levels decrease.

In other words, SU35 is valuable in two aspects: first, when the indicator is lower (higher), the quality of the grape/wine would be expected to increase (decrease); second, it reflects the need for correction approaches (e.g., additional water for cooling grapevines and acidity correction of grape musts and wines) that require more resources.

Due to the systematic bias of the dynamic prediction model (in this case as well), it could happen that the predicted temperatures do not
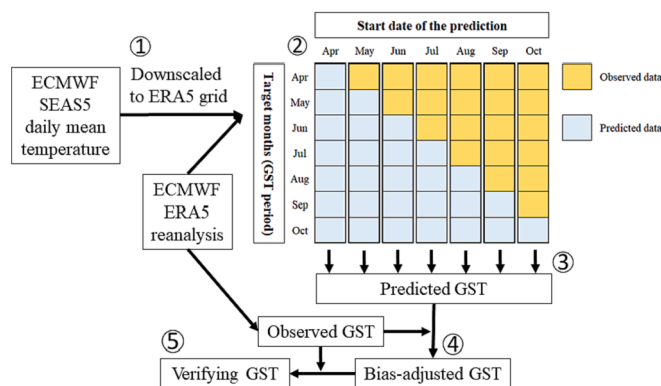

Fig. 2. Flowchart of the general workflow for the blending approach (by taking the GST indicator as an example): (1) regridding SEAS5 predictions to ERA5 grid (from 1° to 0.25°), (2) continuously combining observations and forecasts except for the first start month (i.e., 'Apr' column), (3) computing the GST indicator for each month of the growing season from April to October, (4) applying bias correction and (5) conducting the verification. The inner figure shows step 2: the yellow (blue) squares represent observed (predicted) data, respectively. In detail, since the GST was defined from April to October (i.e., the target months), we first used the prediction issued in April (it lasts until October, see the 'Apr' column) and computed the indicator (i.e., based purely on prediction in this case). In May (see the 'May' column), we then used the predictions issued in May and obtained the indicator based on observations (April) and predictions (from May to October); when the month of June arrived, we combined predictions from June-October and the 2-month observations (April and May) to obtain the indicator. In the last month (see the 'Oct' column) predictions for October and observations from April to September were used for the calculation of the indicator. (For interpretation of the references to colour in this figure legend, the reader is referred to the web version of this article.)

follow the same statistical distribution as that observed. Therefore, instead of using an absolute threshold (e.g., 35 °C for the SU35 indicator), we have worked with the percentile in the prediction that corresponds to the percentile position of the 35 °C value in the observational data. This modification is shown in the formula (see Table s1) and implicitly incorporates a bias correction (Casanueva et al., 2018). The basis of this approach is to compare the percentile corresponding to the predicted (maximum) temperature with the observational percentile corresponding to 35 °C for each day to determine whether the predicted temperature is above the threshold or not. After that, the SU35 indicator can be obtained by summing all the days exceeding the threshold over the 7-month period.

Steps from seasonal forecasts of ECVs toward bioclimatic indicators and the subsequent verification

In order to maximize the adoption of seasonal forecasts in users' decision-making workflows, we introduced the 'blending' approach to all the bioclimatic indicators. By combining observations and forecasts, this key strategy aims to increase users' confidence in the reformed predictions. Each step, from the seasonal forecasts of the variables to the tailored indicators (and the subsequent verification), is described in the following list as well as in Fig. 2 (taking GST as an example).

1. Match the resolutions of datasets (forecast and observation). To this aim, regridding (or other methods of post-processing) could be applied before or after the calculation of an indicator. However, the impact of their sequence on the outcomes has rarely been investigated. Some (Zhang et al., 2011) are in favor of remapping the climatic variable as the first step while others (Diaconescu et al., 2015) compute the indicator before interpolating it to another resolution. It was emphasized that the smoothing of extreme values (Diaconescu
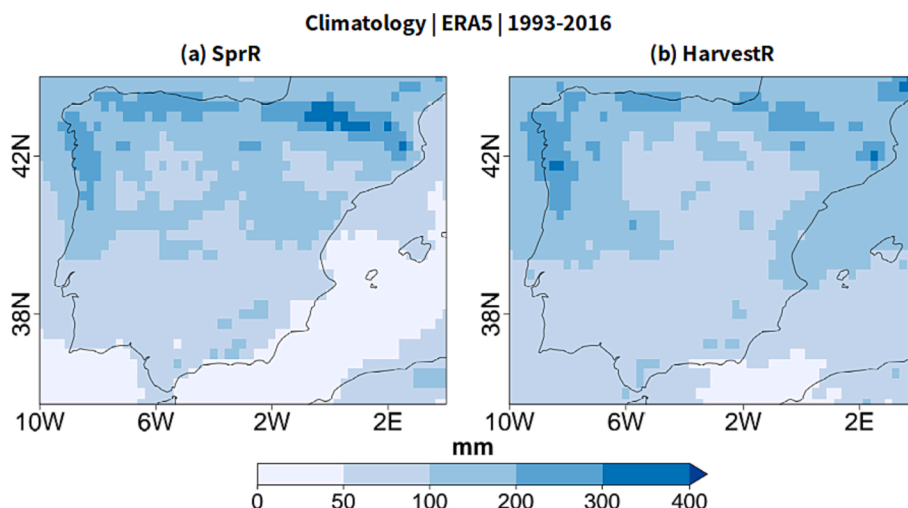
Fig. 3. ERA5 climatology for (a) SprR and (b) HarvestR indicators (accumulated precipitation from 21st April to 21st June and from 21st August to 21st October, respectively) over the Iberian Peninsula considering the 1993–2016 period.

et al., 2015) as well as the comparability between prediction and observation (Zhang et al., 2011) should be taken into account when deciding the order. In this work, the interpolation was applied to the variables (temperature or precipitation) before computing the indicators to avoid the smoothing of extreme values

2. Combination of observations and forecasts ("blending"). The basis for this strategy is that the predictions of ECVs are progressively replaced with observational data as soon as they become available (i. e., when entering the indicator definition period).

3. Computation of the bioclimatic indicators. This was performed with the 'blended' observation-forecast series for each start date considered.

4. Bias correction. Seasonal predictions show biases due to a mixture of uncertainties such as the imperfect initial and boundary conditions, parametrizations of non-resolved phenomena or internal errors, among others (Slingo and Palmer, 2011). Therefore, a bias adjustment has often been required to adjust the forecasts before any practical application. Here, the Simple Bias Correction (SBC hereafter) method (Leung et al., 1999) was applied individually to each grid point (see the formula in the supplementary material).

5. Verification. The variability of the skill metrics obtained in this step indicates the improvement/deterioration seen as the weight of the observations within the indicator increases. In this work, both the ensemble mean Pearson's correlation coefficient (r) and FRPSS have been computed with a cross-validation strategy. The former represents the linear relationship between the data sets, so it is not expected to see a decrease when more observations are included. Furthermore, the decisive month(s) that plays a key role in the indicators could probably be perceived when a marked increased correlation is found. As for the FRPSS, it is a good measure to evaluate the performance of a tercile-based forecast product (commonly used in climate services) when compared to a baseline (i.e., climatology) that also improves as the season progresses (to ensure a fair comparison as well as to understand the added value that this forecasting approach could bring). Specifically, the ensemble climatology data that acted as the baseline reference was generated by resampling ERA5 with the bootstrap (with replacement) and cross-validation (leave-one-out) methods. That is, for the start months from May to October (i.e., May to Oct columns), when computing the FRPSS, the same blending approach was applied to the baseline climatology (i.e., the available observations were combined with the climatology of the remaining months). For instance, for the 'May' column in Fig. 2, the observed April data was combined with the climatology of May-October before calculating the GST baseline for

FRPSS. When the season progressed to October, the observations from April to September were merged with the October climatology for generating the GST baseline. It is worth noting that the (past) observed data could benefit both the baseline climatology as well as the prediction. As a result, the FRPSS is expected to drop over some places in the latter months of the defined period. These cases do not mean that the forecasts worsened the quality, instead, they represent that the blended predictions have not outperformed the blended climatology.

To perform the above steps efficiently, we used three main R packages. Firstly, the CSTools (Pérez-Zanón et al., 2021b) can retrieve the data from netCDF files (and internally regrid it by using the Climate Data Operator developed by Schulzweida, 2020) in addition to applying bias adjustment. Secondly, we used the CSIndicators to combine observations and forecasts before calculating the indicators. Lastly, the computation of the skill metrics was conducted with the easyVerification (MeteoSwiss, 2017). The interoperability of these packages is granted by the fact that the three packages use multidimensional arrays as inputs. Moreover, the functions in CSTools and CSIndicators benefit from multiApply R-package (BSC-CNS et al., 2019) by making them flexible to work with data arrays of any number of dimensions (e. g., to calculate the indicator for station-level or gridded data) and by triggering parallel computation (by simply indicating the required number of cores).

On top of that, the CSIndicators and its sister R-packages within the Climate Forecast Analysis Tools framework (Pérez-Zanón et al., 2021a) simplified the development of climate services by enabling developers to easily compute and analyze the indicators with a high degree of flexibility. For instance, the function PeriodAccumulation(), which calculates the sum of a variable provided in the data array over a user-specified period, was used in this work to compute both SprR and HarvestR thanks to the parameters 'start' and 'end' that permit users to specify the period of interest (e.g., when considering specific grape varieties). Furthermore, users are capable of optimizing the use of their computational resources with the documentation that has been prepared specifically for a wide range of critical agriculture-related indicators (see https://cran.r-project. org/web/packages/CSIndicators/vignettes/AgriculturalIndicators. html).

Results and discussion

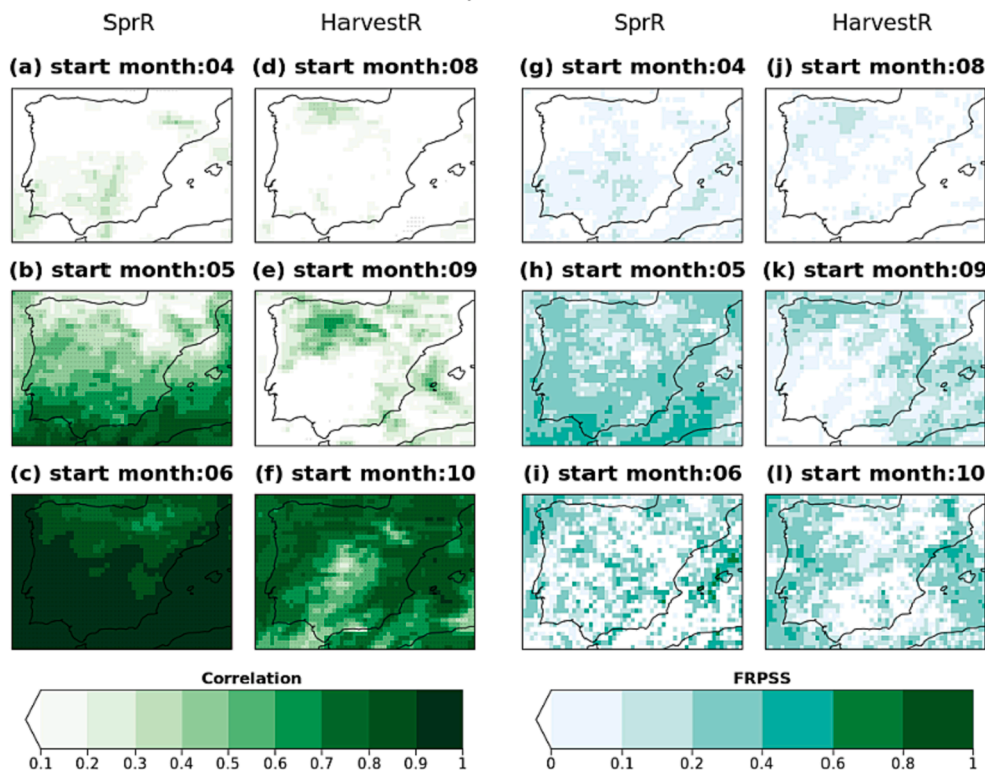Three statistics of the six bioclimatic indicators were shown below

Fig. 4. (a-c & d-f) Ensemble-mean Pearson's correlation coefficient (*r*) and (g-i & j-l) FRPSS for the SprR and HarvestR indicators for the start months from April to June and from August to October, respectively. For the correlation coefficients, the statistical significance has been computed with the one-sided student-T distribution (the points referred to *p*-value below 0.05).

for evaluation: (1) the observational climatology, (2) ensemble-mean Pearson's correlation coefficient and (3) FRPSS (Fricker et al. 2013; Ferro, 2014) of the bias-adjusted predictions. In addition, the remaining bias for all the indicators can be found in the supplementary material (Fig. s1, s2&s4). Taking into account the similarities of the indicators, the results and discussion were grouped into four subsections as below.

Spring total precipitation (SprR) and harvest total precipitation (HarvestR)

Fig. 3 shows that both the SprR and HarvestR indicators have a gradient along the latitude with their maximum values in the northern (especially in the Pyrenees, 300–400 mm/season) and the northwest regions (ranging 200–300 mm/season) of the IP.

The quality and yield of grapes are significantly (usually negatively) influenced by excessive precipitation in the late spring and harvesting periods. For instance, up to one-fourth of the grape yield loss could be caused by precipitation variability as found in a decadal climate-yield relationship study (Agosta et al., 2012). As such, a progressive provision of seasonal forecasts of SprR and HarvestR with improving skills would be helpful for risk management decisions (e.g., spraying against fungal risks due to excess rainfall).

Positive correlations of the start month 04 (08) predictions (see Fig. 4a-c for SprR and Fig. 4d-f for HarvestR) when no observations were included, were limited in the south-central (north-central) IP for SprR (HarvestR), respectively. As the season progressed with more observations being combined, the correlation markedly increased to 0.5–0.7 over wider regions (southern areas for SprR and northern areas for HarvestR) in May (September) and above 0.9 in June (October).

As for their FRPSS (see Fig. 4g-i for SprR and Fig. 4j-l for HarvestR), the areas showing better skills were overall consistent with that of the correlations: up to 0.2 in the southern half (northwestern regions) of the
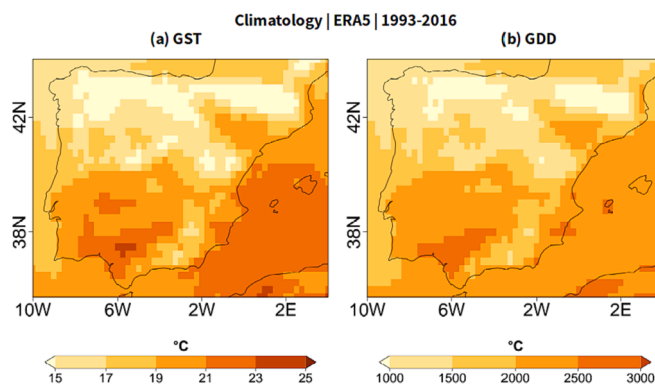

Fig. 5. ERA5 climatology for (a) GST (Growing Season Temperature from April to October) and (b) GDD (Growing Degree Days accumulated from April to October) indicators over the Iberian Peninsula considering the 1993–2016 period.

IP for the start month 04 (08) when only predictions were used. As the observations begin to be included, the FPRSS for SprR shows a widespread increase, reaching 0.2–0.4, for the start month of May. On the other hand, in the start month of September, the increase of FRPSS for HarvestR is relatively constrained to the northern areas. This result is consistent with Crespi et al. (2021) in which a lower RPSS can be seen in the south in SON.

Growing season temperature (GST) and growing degree days (GDD)

These two indicators are positively correlated with each other, thus
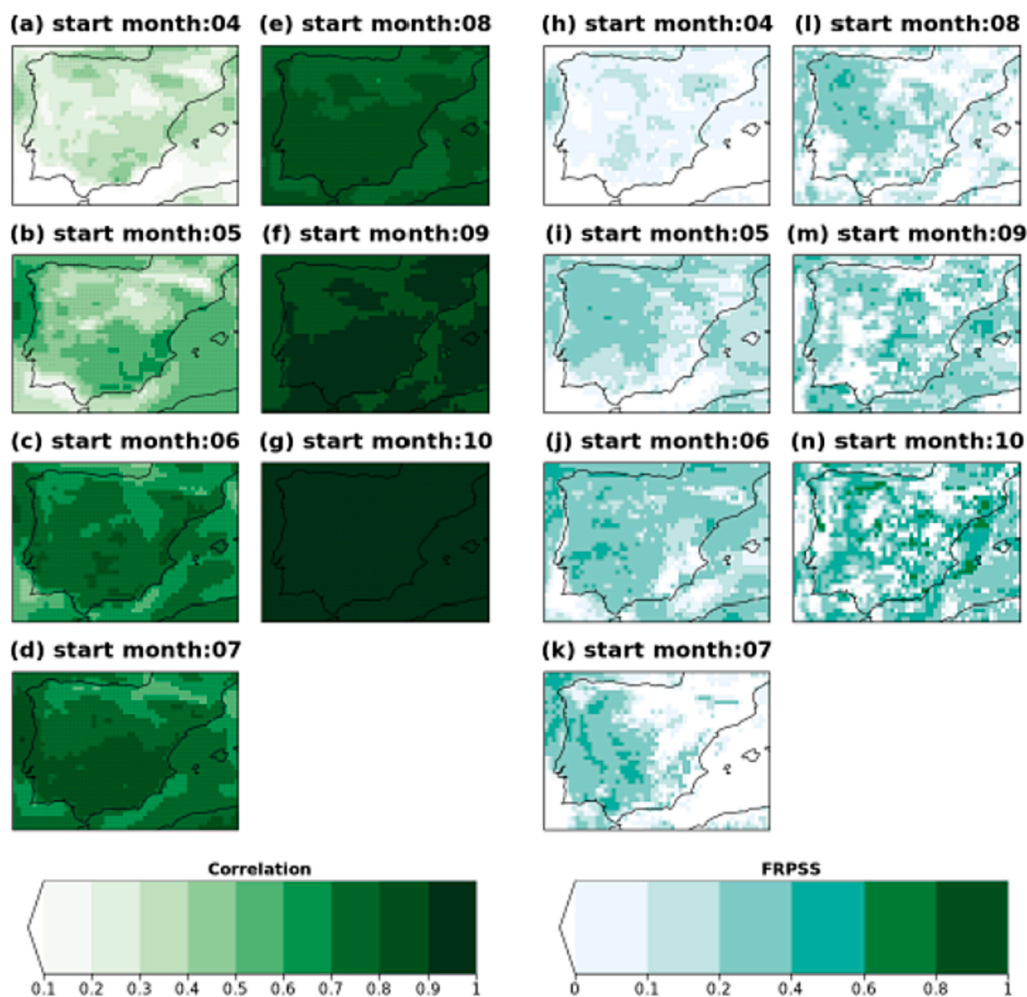
Fig. 6. (a-g) Ensemble-mean Pearson's correlation coefficient (*r*) and (h-n) FRPSS for the GDD indicator for the start months from April to October. For the correlation coefficients, the statistical significance was computed with the one-sided student-T distribution (the points referred to *p*-value below 0.05).

their spatial patterns of climatology are relatively similar. The highest values lie in the south-western areas of the Iberian Peninsula - with GST of above 25 °C and GDD ranging between 2500 °C and 3000 °C - namely the Guadalquivir Valley, the Ebro Valley and the Mediterranean coasts as seen in Fig. 5. The coolest areas are seen in the northern peninsula.

Both skill metrics GST and GDD also show similar spatial patterns and changes. Therefore, only the figures of GDD are shown hereafter (see GST in Fig. s3). Regarding the correlation in April forecasts (no observation included), the values range between 0.2 and 0.5 throughout the IP (except for its southwestern coast). From June onwards, the entire peninsula is covered by correlation coefficients above 0.6 and this skill metric steadily increases until October (fully above 0.9). On the other hand, the change of FRPSS is similar to that of the correlation described. More specifically, the FRPSS shows widespread increases, from 0.4 to 0.6 in the early months such as May and June to above 0.6 in October, Fig. 6h-n. When more observations are combined in the calculation of GDD, it can be seen that in some scattered places there is a decrease in FRPSS (especially from the July start month). This reduction could be partially due to the use of the 'blending' approach in the climatology reference. In fact, as the growing season progresses and the reference begins to include more observations, its performance also improves and, therefore, the FRPSS becomes noisier.

The difference between the smooth spatial patterns of Pearson's correlation coefficients and the irregular patterns of FRPSS could also be a consequence of the relatively larger effect of individual ensemble members in determining the exact collocation of each forecast in the corresponding tercile. For Pearson's correlation coefficient, the signal is dominated by the observation included in the blended indicator. Instead, the computation of FRPSS is based on casting data into terciles, which implies that the use of the tercile thresholds can have a larger sensitivity to the behavior of individual ensemble members that produce random patterns in the skill score.

The magnitude and spatial pattern of GDD obtained in this work are comparable to Fig. 3 of Spinoni et al. (2015) in which the authors emphasized its usefulness in estimating grape production as well as indicating the potential new locations with preferable climate in the forthcoming decades. Moreover, in the management of vineyards, GDD plays an important role in assessing the level of grape maturity, expected wine quality and the timing for harvest (Read et al., 2020) as it well correlates temperature with the plant metabolic processes at different stages of growth such from bud dormancy, flowering, veraison to the harvest (Lombard et al., 2013). Thus, the promising increase in skills from May onwards described above gives more confidence in making a variety of decisions (Lombard et al., 2013) such as estimating the schedules of maturations for the cultivars grown depending on the commercial targets of winemaking as well as planning the labor hirings for the subsequent harvest months especially for the enterprises relying more on part-time labor (Hickey, 2020).
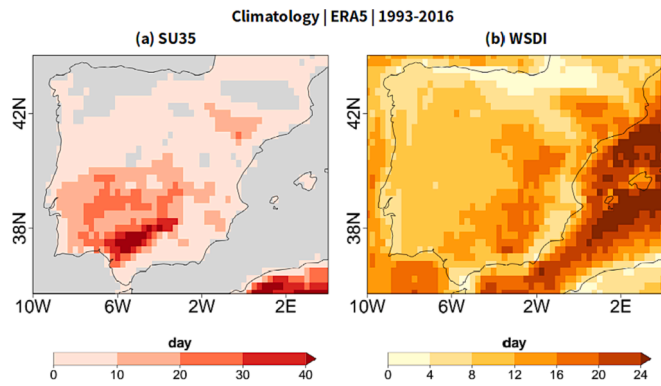
Fig. 7. ERA5 climatology for (a) SU35 (total number of days with daily maximum temperatures above 35 °C from April to October) and (b) WSDI (total number of days counted when 6 consecutive days have maximum temperatures above the temperature corresponding to their 90th percentile from April to October) indicators over the Iberian Peninsula considering the 1993–2016 period. Grey shading indicates grid points that are never above 35 °C in the observation.

Number of heat stress days (SU35)

The SU35 climatology in Fig. 7a shows that the highest values can be found in the Guadalquivir Valley (more than 30 days/season with a maximum of 60 days/season), and the surrounding areas to its north/west (10–30 days/season). In Ebro Valley, the values are up to 20 days while the rest show values below 10. These outcomes are consistent with the station-based work by Fernández-Montes and Rodrigo (2012). Their study, performed with SU30 (an indicator with a 30 °C threshold) over the Iberian Peninsula, reported a similar summer-day distribution (i.e., more hot days in the south) and magnitude (up to 75 days) for the period from 1929 to 2005.

As for its Pearson's correlation coefficient, the predicted SU35 indicator shows limited skill (up to 0.3) in the south-eastern IP in April and May. When the season progresses into June and July (see Fig. 8c&d), the correlation shows a marked increase in the southern half of the IP, with a maximum reaching 0.6 in the Guadalquivir Valley. Furthermore, this correlation continues to increase to more than 0.9 in October across the entire southern half of the peninsula and the Ebro Valley.

As regards FRPSS shown in Fig. 8h-n, positive FRPSS starts to appear in the central, southwestern and southeastern regions of the IP, when the first-month observations are included (i.e., in May). As seen in the correlation, the FRPSS increases from 0.1 to 0.4 to above 0.4 in the southern part of the peninsula from June to August. However, FRPSS remarkably
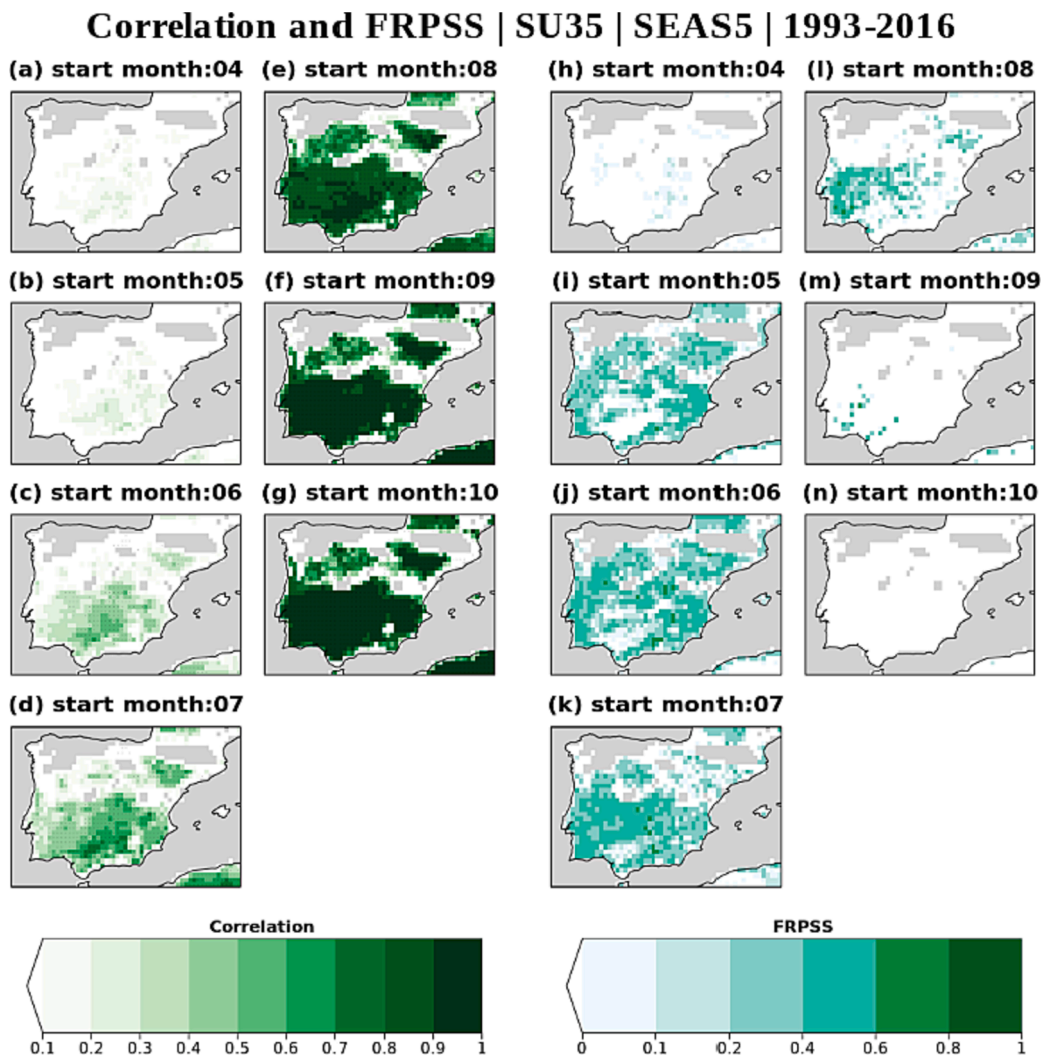

Fig. 8. (a-g) Pearson ensemble-mean correlation (*r*) and (h-n) FRPSS for the SU35 indicator for the start months from April to October. For the correlation coefficients, the statistical significance was computed with the one-sided student-T distribution (the points referred to *p*-value below 0.05).
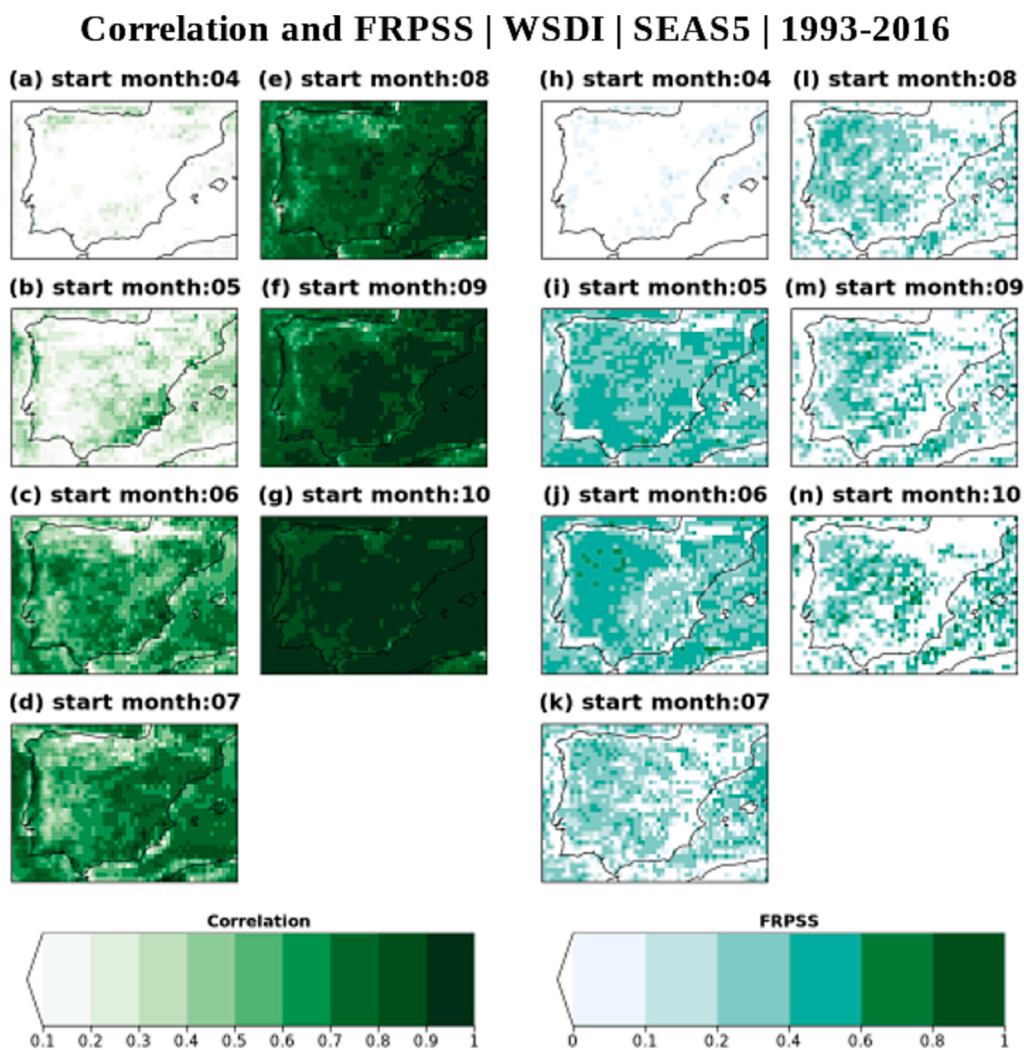
Fig. 9. (a-g) Ensemble-mean Pearson's correlation coefficient (*r*) and (h-n) FRPSS for the WSDI indicator for the start months from April to October. For the correlation coefficients, the statistical significance was computed with the one-sided student-T distribution (the points referred to *p*-value below 0.05).

decreases from September onwards partially because there are fewer hot days after summertime. In addition, this reduction of FRPSS may hint that the inclusion of the key-month (in which most of the hot days occur) observed values in the climatology raised the quality of the reference 'baseline' when computing this skill metric.

The increase in the skill metrics observed for SU35 throughout the season (except for FRPSS in September and October) is important because flowers and grapes are extremely vulnerable to unfavorable heat. Thus, with this information, a number of field interventions could be implemented to improve yield and quality. For instance, an early preparedness of a suitable canopy would adjust the radiation received by berries (Hayman et al., 2009) at the early month of veraison (usually in July and August). Additionally, the timely use of drip irrigation water would cool the vineyard by enhancing evapotranspiration. This strategy would be applied when plants are already in a stress condition (to avoid attaining severe stress) but simultaneously keeping them moderately stressed to favour grape quality.

Warm Spell Duration Index (WSDI)

The spatial pattern of the climatological WSDI (see Fig. 7b) is centred in the eastern interior of the IP, ranging 12–20 days/season while the rest, falls between 8 and 12 days/season. The variability of warming in the vineyard plays a key role in the level of the quality-associated sugar

and flavour compounds (Greer and Weedon 2013), and in turn, determines the need for field intervention and the harvesting date. As such, an advanced skilful estimate of WSDI for the coming months would better inform the relevant decisions including the sunburn and leaf senescence prevention (and the relevant costs required).

The ensemble-mean correlation and FRPSS shown in Fig. 9 are positive but constrained over some of the north-western regions of the IP in April. Nevertheless, it is worthy to remark that the southeast of the peninsula has a correlation up to 0.7 and a widespread increase in FRPSS in May when only one-month observation is included. When the season progresses to June, the correlation remains well above 0.6 and attains values above 0.9 throughout the entire peninsula in October (see Fig. 9c-g). However, the FRPSS increases over the eastern half of the IP in June and the areas with positive values start to decrease slightly and sporadically from July onwards. Still, in the October start month, FRPSS of 0.4–0.8 can be seen in most of the central areas of the studied domain. As explained previously, those reductions in FRPSS could be partially due to the improving baseline set when more observations become available and are combined in the calculation of WSDI.

Conclusions

Regional weather and climate are key elements in the vineyard growth cycle and, hence, in the quality of wines. The IP, home of world-

known wine regions, faces several challenges due to climate change such as an increasing risk of temperature extreme events and unprecedented variability of seasonal rainfall (Viceto et al., 2017).

With the potential value of using seasonal forecasts, this work presented a user-driven approach that could become the basis of future climate services. First, six bioclimatic indicators, which are valuable from the perspective of the wine-sector users, were chosen to assess the effect of the proposed approach on the prediction quality of seasonal forecasts: two (four) precipitation- (temperature-) derived indicators, respectively. Second, the ECMWF SEAS5 predictions were interpolated to ERA5 grid to avoid smoothing the observed extreme values. After that, the new approach aimed to improve the forecasting skill of the predictions by continuously blending the past observations with the latest predictions as the growing season progressed from April to October. Finally, after computing the indicators using the 'blending' ECVs from the previous step, the Simple Bias Correction method was applied for bias-adjustment and followed by the verification.

Remarkably, the 'blending' approach is proven to be of great benefit for seasonal forecast service adoption in view of the fact that increases in both correlation coefficient and FRPSS could be seen from the early stages of the growing season. Regarding the skill of prediction initialized in April (early months of the growing season), the GST and GDD show better skill than the other indicators. Additionally, the higher correlations for GDD in the southern IP as shown in Fig. 6c-e are generally consistent with the spatial pattern of forecasting quality reported before (Crespi et al., 2021).

Regarding precipitation-related indicators, the SprR predictions tended to be more skilful than HarvestR after a one-month observation was included. Besides, concerning their spatial distributions of the skill metrics, the skills are higher for SprR (HarvestR) over the southern (northern) IP as shown in Fig. 4. This difference in the spatial patterns could be associated with the varying qualities of the SEAS5 precipitation in different seasons as indirectly shown in Crespi et al. (2021). In this work, Crespi et al. showed that the correlation in MAM was higher in southern IP, whereas the northern part attained higher correlations in SON.

As for the two heat stress indicators (i.e. SU35 and WSDI), the progressive increase in skill for SU35 is focused on the southern half of the peninsula while the improvement for WSDI is more widespread. Moreover, WSDI starts to be skilful approximately-one month earlier (June, see Fig. 9c&j) than SU35 (July, see Fig. 8d&k).

To sum up, this paper has shown that the adoption of the 'observation-forecast blending approach' on the tailored bioclimatic indicators in seasonal forecast climate services offers a new opportunity to wine-sector users. On top of that, the CSIndicators and its sister R-packages within the Climate Forecast Analysis Tools framework (Pérez-Zanón, 2021a) simplified the development of climate services by enabling developers to easily compute and analyze the indicators with a higher flexibility of these tools.

The systematic assessment carried out throughout all the start dates of the growing season highlights the progressive increase in the forecasting quality that would ultimately allow the user to find the best moment to make a specific decision considering both anticipation and performance. In other words, this work demonstrates the improved performance and leaves the decision of using either skill metric or both to the users according to their needs and decisions. One of the near future works is to prove the transferability by appling this 'blending' strategy to indicators in other areas. Furthermore, it is also worthwhile to keep cooperating with end-users to understand to what extent this strategy could benefit specific decisions in 'real-world' circumstances.

CRediT authorship contribution statement

Chihchung Chou: Formal analysis, Visualization, Investigation, Writing – original draft. **Raül Marcos-Matamoros:** Conceptualization, Investigation, Supervision, Writing – original draft. **Lluís Palma Garcia:** Data curation, Writing – review & editing. **Núria Pérez-Zanón:** Software, Writing – review & editing. **Marta Teixeira:** Writing – review & editing. **Sara Silva:** Writing – review & editing. **Natacha Fontes:** Writing – review & editing. **Antonio Graça:** Writing – review & editing. **Alessandro Dell'Aquila:** Methodology, Writing – review & editing. **Sandro Calmanti:** Methodology. **Nube González-Reviriego:** Conceptualization, Supervision.

Declaration of Competing Interest

The authors declare that they have no known competing financial interests or personal relationships that could have appeared to influence the work reported in this paper.

Data availability

Data will be made available on request.

Appendix A. Supplementary data

Supplementary data to this article can be found online at https://doi.org/10.1016/j.cliser.2023.100343.

References

Agosta, E., Canziani, P., Cavagnaro, M., 2012. Regional climate variability impacts on the annual grape yield in Mendoza, Argentina. J. Appl. Meteorol. Climatol. 51, 993–1009. https://doi.org/10.1175/JAMC-D-11-0165.1.

Bandhauer, M., Isotta, F., Lakatos, M., Lussana, C., Båserud, L., Izsák, B., Frei, C., 2022. Evaluation of daily precipitation analyses in E-OBS (v19. 0e) and ERA5 by comparison to regional high-resolution datasets in European regions. Int. J. Climatol. 42 (2), 727–747. https://doi.org/10.1002/joc.7269.

Blanco-Ward, D., et al., 2019. Climate change potential effects on grapevine bioclimatic indices: A case study for the Portuguese demarcated Douro Region (Portugal). BIO Web Conf. 12, 01013. https://doi.org/10.1051/bioconf/20191201013.

BSC-CNS, Manubens, N. and Hunter, A.: Apply Functions to Multiple Multidimensional Arrays or Vectors, [online] Available from: https://cran.r-project.org/package=multiApply, 2019.

Camps, J.O., Ramos, M.C., 2012. Grape harvest and yield responses to inter-annual changes in temperature and precipitation in an area of north-east Spain with a Mediterranean climate. Int. J. Biometeorol. 56, 853–864. https://doi.org/10.1007/s00484-011-0489-3.

Casanueva, A., Bedia, J., Herrera, S., Fernández, J., Gutiérrez, J.M., 2018. Direct and component-wise bias correction of multi-variate climate indices: the percentile adjustment function diagnostic tool. Clim. Change 147, 411–425. https://doi.org/10.1007/s10584-018-2167-5.

Comité Européen des Entreprises Vins, 2015: EUROPEAN WINE: a solid pillar of the European Union economy. https://www.ceev.eu/wp-content/uploads/2019/11/Brochure_CEEV_-_High_resolution.pdf (Accessed May 25, 2021).

Crespi, A., Petitta, M., Marson, P., Viel, C., Grigis, L., 2021. Verification and bias adjustment of ECMWF SEAS5 seasonal forecasts over europe for climate service applications. Climate 9 (12), 181. https://doi.org/10.3390/cli9120181.

Danielson, J.J., Gesch, D.B., 2011, Global multi-resolution terrain elevation data 2010 (GMTED2010): U.S. Geological Survey Open-File Report 2011–1073, 26 p.

Diaconescu, E.P., Gachon, P., Laprise, R., 2015. On the remapping procedure of daily precipitation statistics and indices used in regional climate model evaluation. J. Hydrometeorol. 16, 2301–2310. https://doi.org/10.1175/JHM-D-15-0025.1.

Diffenbaugh, N.S., et al., 2017. Quantifying the influence of global warming on unprecedented extreme climate events. Proc. Natl. Acad. Sci. 114, 4881–4886. https://doi.org/10.1073/pnas.1618082114.

Doblas-Reyes, F.J., García-Serrano, J., Lienert, F., Biescas, A.P., Rodrigues, L.R.L., 2013. Seasonal climate predictability and forecasting: status and prospects. Wiley Interdiscip. Rev. Clim. Chang. 4, 245–268. https://doi.org/10.1002/WCC.217.

Emerton, R., et al., 2018. Developing a global operational seasonal hydro-meteorological forecasting system: GloFAS-Seasonal v1.0. Geosci. Model Dev. 11, 3327–3346. https://doi.org/10.5194/gmd-11-3327-2018.

Fernández-Montes, S., Rodrigo, F.S., 2012. Trends in seasonal indices of daily temperature extremes in the Iberian Peninsula, 1929–2005. Int. J. Climatol. 32 (15), 2320–2332. https://doi.org/10.1002/joc.3399.

Ferro, C.A.T., 2014. Fair scores for ensemble forecasts. Quart. J. Roy. Meteor. Soc. 140, 1917–1923. https://doi.org/10.1002/qj.2270.

Fischer, E.M., Seneviratne, S.I., Vidale, P.L., Lüthi, D., Schär, C., 2007. Soil moisture–atmosphere interactions during the 2003 European summer heat wave. J. Clim. 20 (20), 5081–5099. https://doi.org/10.1175/JCLI4288.1.

Fontes, N., J. Martins, and A. Graça, 2016: Study of agrometeorological measurements on "Terroirs" of Alentejo wine region: impact on grape yield and harvest date variation. https://www.researchgate.net/profile/Antonio_Graca/publication/304062918_STUDY_OF_AGROMETEOROLOGICAL_MEASUREMENTS_ON_TERROIRS_OF_ALENTEJO_WINE_REGION_IMPACT_ON_GRAPE_YIELD_AND_HARVEST_DATE_VARIATION/links/576538c808ae1658e2f48c61/STUDY-OF-AGROMETEOROLOGIC.

Fraga, H., Malheiro, A.C., Moutinho-Pereira, J., Cardoso, R.M., Soares, P.M.M., Cancela, J.J., Pinto, J.G., Santos, J.A., 2014a. Integrated analysis of climate, soil, topography and vegetative growth in iberian viticultural regions. PLoS One 9. https://doi.org/10.1371/JOURNAL.PONE.0108078.

Fraga, H., Malheiro, A.C., Moutinho-Pereira, J., Jones, G.V., Alves, F., Pinto, J.G., Santos, J.A., 2014b. Very high resolution bioclimatic zoning of Portuguese wine regions: Present and future scenarios. Reg. Environ. Chang. 14, 295–306. https://doi.org/10.1007/s10113-013-0490-y.

Fricker, T.E., Ferro, C.A.T., Stephenson, D.B., 2013. Three recommendations for evaluating climate predictions. Meteor. Appl. 20, 246–255. https://doi.org/10.1002/met.1409.

Giuliani, M., Crochemore, L., Pechlivanidis, I., Castelletti, A., 2020. From skill to value: isolating the influence of end user behavior on seasonal forecast assessment. Hydrol. Earth Syst. Sci. 24, 5891–5902. https://doi.org/10.5194/hess-24-5891-2020.

Goodess, C.M., Jones, P.D., 2002. Links between circulation and changes in the characteristics of Iberian rainfall. Int. J. Climatol. 22 (13), 1593–1615. https://doi.org/10.1002/joc.810.

Greer, D.H., Weedon, M.M., 2013. The impact of high temperatures on Vitis vinifera cv. Semillon grapevine performance and berry ripening. Front. Plant Sci 4, 491. https://doi.org/10.3389/fpls.2013.00491.

Gubler, S., et al., 2020. Assessment of ECMWF SEAS5 seasonal forecast performance over South America. Weather Forecast. 35, 561–584. https://doi.org/10.1175/WAF-D-19-0106.1.

Hansen, J.W., Mason, S.J., Sun, L., Tall, A., 2011. Review of seasonal climate forecasting for agriculture in sub-Saharan Africa. Exp. Agric. 47, 205–240. https://doi.org/10.1017/S0014479710000876.

Hayman, P., MCarthy, M.G., Grace, W., 2009. Assessing and managing the risk of heatwaves in SE Australian wine regions. Aust. N.Z. Grapegrow. Winemak. 543, 22–24.

[dataset] Hersbach, H., and Coauthors, 2020: The ERA5 global reanalysis. Q. J. R. Meteorol. Soc., 146, 1999–2049, 10.1002/qj.3803.

Hersbach, H., Bell, B., Berrisford, P., Biavati, G., Horányi, A., Muñoz Sabater, J., Nicolas, J., Peubey, C., Radu, R., Rozum, I., Schepers, D., Simmons, A., Soci, C., Dee, D., Thépaut, J-N. (2018): ERA5 hourly data on pressure levels from 1979 to present. Copernicus Climate Change Service (C3S) Climate Data Store (CDS). (Accessed on < 17-02-2020 >), 10.24381/cds.bd0915c6.

Hickey, C., 2020: Harvest decisions and the complexity thereof, Harvest decisions and the complexity thereof. https://psuwineandgrapes.files.wordpress.com/2020/09/harvest-decisions-and-the-complexity-thereof_extra-text_final-1.pdf.

[dataset] Johnson, S. J., and Coauthors, 2019: SEAS5: The new ECMWF seasonal forecast system. Geosci. Model Dev., 12, 1087–1117, 10.5194/gmd-12-1087-2019.

Jones, G.V., Alves, F., 2012. Impact of climate change on wine production: A global overview and regional assessment in the douro valley of Portugal. Int. J. Glob. Warm. 4, 383–406. https://doi.org/10.1504/IJGW.2012.049448.

Jones, G.V., Davis, R.E., 2000. Using a synoptic climatological approach to understand climate–viticulture relationships. Int. J. Climatol. 20 (8), 813–837. https://doi.org/10.1002/1097-0088(20000630)20:8<813::AID-JOC495>3.0.CO;2-W.

Jones, G. V., and Coauthors, 2005: Changes in European winegrape phenology and relationships with climate. XIV Int. GESCO Vitic. Congr. Geisenheim, Ger. 23-27 August, 2005, 54–61.

Karoglan, M., et al., 2018. Classification of Croatian winegrowing regions based on bioclimatic indices. E3S Web Conf. 50, 1–5. https://doi.org/10.1051/e3sconf/20185001032.

Koufos, G., Mavromatis, T., Koundouras, S., Fyllas, N.M., Jones, G.V., 2014. Viticulture-climate relationships in Greece: The impacts of recent climate trends on harvest date variation. Int. J. Climatol. 34, 1445–1459. https://doi.org/10.1002/joc.3775.

Leung, L.R., Hamlet, A.F., Lettenmaier, D.P., Kumar, A., 1999. Simulations of the ENSO Hydroclimate Signals in the Pacific Northwest Columbia River Basin. Bull. Am. Meteorol. Soc. 80, 2313–2330. https://doi.org/10.1175/1520-0477(1999)080<2313:SOTEHS>2.0.CO;2.

Lombard, K., Maier, B., Thomas, J.F., O'Neill, M., Allen, S., Heyduck, R., 2013. Wine grape cultivar performance in the Four Corners Region of New Mexico in 2010–12. HortTechnology 23 (5), 699–709. https://doi.org/10.21273/HORTTECH.23.5.699.

Malheiro, A.C., Santos, J.A., Fraga, H., Pinto, J.G., 2010. Climate change scenarios applied to viticultural zoning in Europe. Clim. Res. 43, 163–177. https://doi.org/10.3354/cr00918.

Manzanas, R., Gutiérrez, J.M., Bhend, J., Hemri, S., Doblas-Reyes, F.J., Torralba, V., Penabad, E., Brookshaw, A., 2019. Bias adjustment and ensemble recalibration methods for seasonal forecasting: a comprehensive intercomparison using the C3S dataset. Clim. Dyn. 53, 1287–1305. https://doi.org/10.1007/s00382-019-04640-4.

Marcos-Matamoros, R., Llasat, M.C., Quintana-Seguí, P., Turco, M., 2017. Seasonal predictability of water resources in a Mediterranean freshwater reservoir and assessment of its utility for end-users. Sci. Total Environ. 575, 681–691. https://doi.org/10.1016/J.SCITOTENV.2016.09.080.

Marcos-Matamoros, R., González-Reviriego, N., Graça, A., Dell'Aquila, A., Vigo, I., Silva, S., Sanderson, M., 2020. Second Feedback report from users on wine pilot service development. Zenodo. https://doi.org/10.5281/zenodo.5710836.

Meehl, G.A., Tebaldi, C., 2004. More intense, more frequent, and longer lasting heat waves in the 21st century. Science 305 (5686), 994–997. https://doi.org/10.1126/science.1098704.

MeteoSwiss: easyVerification: Ensemble Forecast Verification for Large Data Sets, CRAN [online] Available from: https://cran.r-project.org/package=easyVerification, 2017.

OIV, 2016: OIV - International Organisation of Vine and Wine. https://www.oiv.int/ (Accessed May 25, 2021).

Pérez-Zanón, N., L.-P. Caron, C. Alvarez-Castro, L. Batte, J. von Hardenberg, L. LLedó, N. Manubens, E. Sánchez-Garcia, B. van Schaeybroeck, V. Torralba, and D. Verfaillie, 2021b: CSTools: Assessing Skill of Climate Forecasts on Seasonal-to-Decadal Timescales. R package version 4.0.1. Available from: https://CRAN.R-project.org/package=CSTools doi: https://zenodo.org/record/5549474#.YXK3fdlBYqB.

Pérez-Zanón, N., C. Chihchung, and L. Lledó, 2021c: CSIndicators: Sectoral Indicators for Climate Services Based on Sub-Seasonal to Decadal Climate Predictions, CRAN [online] Available from: https://cran.r-project.org/package=CSIndicators.

Pérez-Zanón, N., 2021a: Climate Forecast Analysis Tools Framework (8th BSC Doctoral Symposium 2021, online, 13th May 2021) Available from: https://www.bsc.es/sites/default/files/public/8th_bsc_so_doctoral_symposium_book_of_abstracts.pdf.

Petrie, P.R., Sadras, V.O., 2008. Advancement of grapevine maturity in Australia between 1993 and 2006: Putative causes, magnitude of trends and viticultural consequences. Aust. J. Grape Wine Res. 14, 33–45. https://doi.org/10.1111/j.1755-0238.2008.00005.x.

Raoult, B., Bergeron, C., López Alós, A., Thépaut, J.-N., Dee, D., 2017. Climate service develops user-friendly data store. ECMWF newsletter 151, 22–27. https://doi.org/10.21957/p3c285.

Read, P. E., Loseke, B. A., Gamet, S. J., 2020 Relating harvest timing to growing degree accumulation in grapes. Acta Hortic. 1274, 109-112, 10.17660/ActaHortic.2020.1274.13.

Rodrigo, F.S., 2021. Exploring combined influences of seasonal East Atlantic (EA) and North Atlantic Oscillation (NAO) on the temperature-precipitation relationship in the Iberian Peninsula. Geosciences 11 (5), 211. https://doi.org/10.3390/geosciences11050211.

M. Sanderson,, C. Giannakopoulos,, Alessandro Dell'Aquila,, Luigi Ponti,, Sandro Calmanti,, A Graca,, M. Pasqui,, J. lopez, A. Toreti. (2019). Assessment of quality of European climate observations and their appropriateness for use in climate services for each sector. Zenodo. 10.5281/zenodo.3257503.

Sanderson, Michael and Teixeira, Marta and Fontes, Natacha and Silva, Sara and GRAÇA, ANTONIO, 2022, The Risk of Unprecedented High Rainfall in Wine Regions of Northern Portugal. SSRN, doi: 10.2139/ssrn.4130788.

Schulzweida, Uwe. (2020, October 31). CDO User Guide (Version 1.9.9). Zenodo. doi: 10.5281/zenodo.4246983.

Slingo, J., Palmer, T., 2011. Uncertainty in weather and climate prediction. Philos. Trans. R. Soc. A Math. Phys. Eng. Sci. 369, 4751–4767. https://doi.org/10.1098/RSTA.2011.0161.

Soares, B.M., Marcos-Matamoros, R., Teixeira, M., Fontes, N., Graça, A., 2019. First feedback report from users on wine pilot service development. Zenodo. https://doi.org/10.5281/zenodo.5710840.

Toit, W.D., Pretorius, I.S., 2002. The occurrence, control and esoteric effect of acetic acid bacteria in winemaking. Ann. Microbiol. 52, 155–179.

Tomasi, D., Jones, G.V., Giust, M., Lovat, L., Gaiotti, F., 2011. Grapevine phenology and climate change: relationships and trends in the veneto region of Italy for 1964–2009. Am. J. Enol. Vitic. 62, 329–339. https://doi.org/10.5344/ajev.2011.10108.

Torralba, V., Doblas-Reyes, F.J., MacLeod, D., Christel, I., Davis, M., 2017. Seasonal climate prediction: a new source of information for the management of wind energy resources. J. Appl. Meteorol. Climatol. 56, 1231–1247. https://doi.org/10.1175/JAMC-D-16-0204.1.

Trigo, R.M., Pozo-Vázquez, D., Osborn, T.J., Castro-Díez, Y., Gámiz-Fortis, S., Esteban-Parra, M.J., 2004. North Atlantic Oscillation influence on precipitation, river flow and water resources in the Iberian Peninsula. Int. J. Climatol. 24 (8), 925–944. https://doi.org/10.1002/joc.1048.

Vajda, A., Hyvärinen, O., 2020. Development of seasonal climate outlooks for agriculture in Finland. Adv. Sci. Res. 17, 269–277. https://doi.org/10.5194/asr-17-269-2020.

Venios, X., Korkas, E., Nisiotou, A., Banilas, G., 2020. Grapevine responses to heat stress and global warming. Plants 9, 1–15. https://doi.org/10.3390/plants9121754.

Viceto, C., Marta-Almeida, M., Rocha, A., 2017. Future climate change of stability indices for the Iberian Peninsula. Int. J. Climatol. 37, 4390–4408. https://doi.org/10.1002/joc.5094.

Vidale, P.L., Lüthi, D., Wegmann, R., Schär, C., 2007. European summer climate variability in a heterogeneous multi-model ensemble. Clim Change 81, 209–232. https://doi.org/10.1007/s10584-006-9218-z.

Weisheimer, A., D. J. Befort, D. MacLeod, T. Palmer, C. O'Reilly, K. Strømmen, 2021: Seasonal forecasts of the twentieth century. Bull. Am. Meteorol. Soc., 101, E1413–E1426, 10.1175/BAMS-D-19-0019.1.

Winsemius, H.C., Dutra, E., Engelbrecht, F.A., Archer Van Garderen, E., Wetterhall, F., Pappenberger, F., Werner, M.G.F., 2014. The potential value of seasonal forecasts in a changing climate in southern Africa. Hydrol. Earth Syst. Sci. 18, 1525–1538. https://doi.org/10.5194/hess-18-1525-2014.

Xu, X., Frey, S.K., Boluwade, A., Erler, A.R., Khader, O., Lapen, D.R., Sudicky, E., 2019. Evaluation of variability among different precipitation products in the Northern Great Plains. Journal of Hydrology. Reg. Stud. 24 (100608) https://doi.org/10.1016/j.ejrh.2019.100608.

Zhang, X., Alexander, L., Hegerl, G.C., Jones, P., Tank, A.K., Peterson, T.C., Trewin, B., Zwiers, F.W., 2011. Indices for monitoring changes in extremes based on daily temperature and precipitation data. Wiley Interdiscip. Rev. Clim. Chang. 2, 851–870. https://doi.org/10.1002/wcc.147.